J. Korean Soc. Appl. Biol. Chem. **54**(6), 852-859 (2011)

Article

Proteomic Analysis of Hepatotoxicity Induced by Titanium Nanoparticles in Mouse Liver

Yu-Mi Jeon, Seul-Ki Park, and Mi-Young Lee*

Department of Medical Biotechnology, SoonChunHyang University, Asan, Chungnam 336-600, Republic of Korea

Received July 20, 2011; Accepted October 11, 2011

Differentially expressed proteins in mouse liver caused by toxicity of titanium nanoparticles (TiO_2 NPs) were screened. More than 1,400 protein spots in mouse liver were detected by two-dimensional gel electrophoresis, and 15 proteins that showed greater than 2-fold expressional changes in response to TiO_2 NPs were identified by liquid chromatography-tandem mass spectrometry. Of these, 12 proteins were down-regulated and 3 proteins were up-regulated upon treatment with TiO_2 NPs. The 15 differentially expressed proteins could be used for detection of inflammation, apoptosis, and antioxidative reaction for treatment of acute hepatic damage by TiO_2 NPs.

Key words: liver, mouse, proteomics, titanium nanoparticles, toxicity

Nanoparticles have been used in a variety of applications such as electrical, industrial, agricultural, and medical applications due to their special properties. However, increasing evidence suggests that the physicochemical properties of the nanoparticles pose potential toxic effects to human health and the environment [Sohaebuddin *et al*., 2010]. The toxicity of nanoparticles is thought to be associated with their small size and high specific surface area. Nanoparticles are expected to be more toxic than bulk particles due to their greater surface reactivity, mobility, and potentially enhanced uptake across biological membranes [Xiong *et al*., 2011].

Titanium dioxide nanoparticles (TiO_2 NPs) have been generally accepted to be low risk to human, because they are chemically and thermally stable [Xu *et al*., 2010]. However, wide spread applications of TiO_2 NPs have already led to an increased concern about the enormous potential for human exposure and environmental release.

Recent studies have unequivocally shown that exposure to TiO_2 NPs produce oxidative damages and hepatocyte necrosis [Linnainmaa *et al*., 1997]. The enhancement of lipid peroxides in the mouse liver by TiO_2 NPs implicated an oxidative attack activated by a reduction of the antioxidative defense mechanism and caused DNA cleavage of the mouse liver [Ma *et al*., 2009; Cui *et al*., 2010]. Exposure to high levels of TiO_2 NPs was associated with the induction of tumors in a few animal studies [Park *et al*., 2009]. The hepatocyte apoptosis induced by TiO_2 NPs has been also demonstrated [Wang *et al*., 2007].

However, information on the proteomic alterations associated with hepatotoxicity by TiO_2 NPs at the molecular and cellular levels is not available. Therefore, the differentially expressed proteins by TiO_2 NPs in mouse liver via proteomic approach was investigated to better understand the molecular mechanism underlying hepatotoxicity by TiO_2 NPs at the protein level.

Materials and Methods

Experimental animals. Male ICR mice (7-week-old, weighing 18±2 g) were kept in a separate animal room on a 12 h light-dark cycle, with room temperature maintained at 20±2°C and relative humidity at 60±10%. Commercial TiO_2 NPs (Sigma-Aldrich, St. Louis, MO), composed of the crystallographic form of TiO_2 (anatase) and with an average diameter of <25 nm, were mixed with phosphate buffered saline (PBS) and then ultrasonicated for 10 min. Male ICR mice were randomly assigned to control and treatment groups (n=3). Animals in the treatment group were injected intraperitoneally with 138 mg/kg body weight of TiO_2 NPs suspension. At 30 min post-injection, 100 μL (1 mg) of TiO_2 NP suspension was instilled nasally every day for 7 days. After 7 days, all animals were anaesthetized with ether and sacrificed, and their

*Corresponding author
Phone: +82-41-530-1355; Fax: +82-41-530-1355
E-mail: miyoung@sch.ac.kr

http://dx.doi.org/10.3839/jksabc.2011.130

livers were harvested and stored at –70°C.

Sample preparation for proteomic analysis. Liver tissues were snap frozen in liquid N_2 and stored at −70°C until analysis. The frozen liver tissue samples (100 mg) were homogenized in a rehydration buffer containing 7 M urea, 2 M thiourea, 4.5% (w/v) 3-[(3-cholamidopropyl) dimethylammonio]-1-propanesulfonate (CHAPS), 40 mM Tris, 100 mM 1,4-dithioerythritol (DTE), 0.25% immobilized pH gradient (IPG) buffer (pH 3-10), and protease inhibitor cocktail. Solubilized tissue was centrifuged (12,000 g, 30 min, 4°C), and the resulting supernatant fractions were analyzed by two-dimensional (2-DE) gel electrophoresis [Park *et al*., 2011].

2-DE gel electrophoresis. For the first-dimensional electrophoresis of proteins, a fixed amount of 1 mg protein samples were loaded onto 24-cm IPG strips (Immobiline™ DryStrip, Amersham Biosciences, Uppsala, Sweden) from GE Healthcare (Fairfield, CA) with a nonlinear (NL) pH 3−10 gradient range. The strip was rehydrated in a buffer [7 M urea, 2 M thiourea, 4.5% (w/v) CHAPS, 40 mM Tris, 100 mM DTE and protease inhibitor cocktail], mixed with 0.25% IPG solution (pH 3−10), and separately loaded onto a first-dimension IPG strips and focused through electrophoresis for a total of 84 kVh at 20°C. Focusing was performed through the following steps: rehydration for 12 h, 200 V/200 Vh, 500 V/500 Vh, 1,000 V/1,000 Vh, 8,000 V/13,500 Vh, and 8,000 V/100,000 Vh. After isoelectric focusing, the strips were treated with equilibration buffer [6 M urea, 2% (w/v) sodium dodecyl sulfate (SDS), 20% (v/v) glycerol, 5 mM tributylphosphine, 2.5% acrylamide, 0.01% bromophenol blue, 0.375 M Tris-HCl, pH 8.8] twice and then soaked for 20 min. The second-dimension separation, SDS-polyacrylamide gel electrophoresis (PAGE), was performed using 8−16% gradient polyacrylamide gels without stacking gels. Proteins were separated by electrophoresis at 10°C for 2 h at 5 mA/gel and then at 18 mA/gel. Electrophoresis was stopped when the dye front began to diffuse from the gel. After electrophoresis, the gels were stained with Brilliant Blue R-250 and then destained in 1% (v/v) acetic acid. Protein spot detection and 2-DE pattern matching were carried out using ImageMaster 2D Platinum software (GE Healthcare). At least three gels for each group were evaluated. To assess differences in spot quantity among the control and treatment groups initially, the two master gels were compared prior to testing [Jeon *et al*., 2010; 2011].

Liquid chromatography-tandem mass spectrometry (LC-MS/MS). Differentially expressed protein spots by TiO_2 nanoparticles in mouse liver were identified using LC-MS/MS. For each experiment, 10 μL of sample was loaded by the auto sampler onto a C_{18} trap column (I.d 300 mm, length 5 mm, particle size 5 mm) for desalting at a flow rate of 20 μL/min. The trapped peptides were then back-flushed and separated on a homemade microcapillary column (150 mm in length) packed with C_{18} resin in 75-μm silica tubing. The spots of interest were excised from the 2-DE gels, destained, dried, and in-gel digested for 2 h at 37°C in a solution containing both trypsin and a protease mixture. An electrospray ionization ion trap mass spectrometer (LCQ Deca XP; Thermo Finnigan, San Jose, CA) was used for peptide detection. The positive ion mode was selected, and the spray voltage was set to 2.5 kV. The spray temperature for analyzing peptides was set to 150°C. Mass spectrometer scan functions and HPLC solvent gradients were controlled using the Xcalibur data system (Thermo Finnigan). MS/MS mass peak lists were analyzed for *b* and *y* ions using SEQUEST (version 3.3.1, Thermo Finnigan) software. SEQUEST was used to match MS/MS spectra to peptide with MASCOT MS/MS ion search tool using the Swiss-Prot 49.1 database [Passadore *et al*., 2009].

Western blotting. TiO_2 NPs-exposed liver tissues were solubilized in ice-cold extraction buffer for 10 min at 4°C and then centrifuged at 12,000 × g for 30 min. Total proteins were resolved on 10% SDS-PAGE gels, transferred onto polyvinylidene difluoride (PVDF) membranes, blocked for 2 h in blocking solution. They were then incubated overnight with individual antibody at 4°C and then with horseradish peroxidase-conjugated secondary antibody for 1 h at room temperature. The membranes were visualized using the enhanced chemiluminescence plus Western blotting detection system (Amersham Biosciences, Piscataway, NJ). Intensity of the bands was analyzed using ImageQuant TL software (Amersham Biosciences, Arlington Heights, IL).

Blood biomarker assay. The blood serum was obtained by centrifugation of the whole blood at 2,500 rpm for 20 min. Liver function was evaluated based on serum levels of aspartate aminotransferase (AST), alanine aminotransferase (ALT), and alkaline phosphatase (ALP). All biochemical parameters were performed using a clinical automatic chemistry analyzer (Roche Diagnostics, Lewes, UK). For statistical analysis, data are presented as the mean ± SD. Comparisons between groups were performed using one-way analysis of variance (ANOVA), followed by Duncan's multiple range test. $p < 0.05$ was considered statistically significant.

Antioxidant enzyme activity on the gel. The antioxidant machinery of liver tissue was analyzed by determining catalase (CAT) and superoxide dismutase (SOD) on the native-PAGE. Liver extract was centrifuged at 12,000 rpm for 25 min at 4°C, and the supernatant was used for antioxidant enzyme analysis. Aliquots of 100 μg

Table 1. Changes in the biochemical parameters of mouse serum by TiO_2 NPs

Groups	ALT (U/L)	AST (U/L)	ALP (U/L)
Control	23±2.2	50±3.0	43±5.6
TiO_2 NPs	30±2.3*	57±1.2*	63±7*

*p <0.05 significant difference comparing with the control group

ALT, alanine aminotransferase; AST, aspartate aminotransferase; ALP, alkaline phosphatase, Values represent means ± SD

protein extracts from the liver tissue were applied to native PAGE. After the separation, the gel was stained for individual enzyme activities.

Results

Biochemical parameters in serum. Table 1 lists the changes in biochemical parameters, such as AST, ALT, and ALP, in the sera of mice induced by TiO_2 NPs. The levels of the hepatic enzymes of AST, ALT and ALP in the sera increased after exposure to TiO_2 NPs.

Proteomic analysis of the differentially expressed proteins by TiO_2 NPs. Approximately 1,400 protein spots were detected on the 2-DE. Figure 1 shows 2-DE images of mouse liver proteins following exposure to TiO_2 NPs. After comparing 2-DE protein patterns on duplicate gels, 15 spots with notable changes between the control and TiO_2 NPs-exposed groups were successfully identified (Table 2). Of these, 12 displayed reduced intensities in TiO_2 NP-exposed livers, and 3 showed increased intensities (Fig. 2). The down-regulated proteins were fructose-1,6-bisphosphatase 1 (spot 2), propionyl-CoA carboxylase alpha chain (spot 3), electron transfer flavoprotein-uiquinone oxidoreductase mitochondrial precursor (spot 4), carbonic anhydrase 2 (spot 5), sulfite oxidase mitochondrial precursor (spot 6), arginase-1 (spot 7), aldehyde dehydrogenase (ALDH) family 8 member A1 (spot 8), CAT (spot 9), elongation factor 1-alpha (spot 10), 2 of cytochrome b-c1 complex subunit 1 mitochondrial precursor (spots 11 and 15), and apolipoprotein A-1 precursor (spot 12). The up-regulated proteins were isoform 1 of 60 kDa heat shock protein (HSP) mitochondrial precursor (spot 1), isovaleryl-CoA dehyrogenase mitochondrial precursor (spot 13) and beta-ureidopropionase (spot 14). The zoom-up views of the differentially expressed proteins by TiO_2 NPs are shown in Fig. 2.

Validation by Western blotting. From the identified protein spots, 60 kDa HSP was selected for Western blot analysis (Fig. 3). The result indicated that HSP60 was expressed at low level in control, but was present at higher levels after TiO_2 NPs treatment.

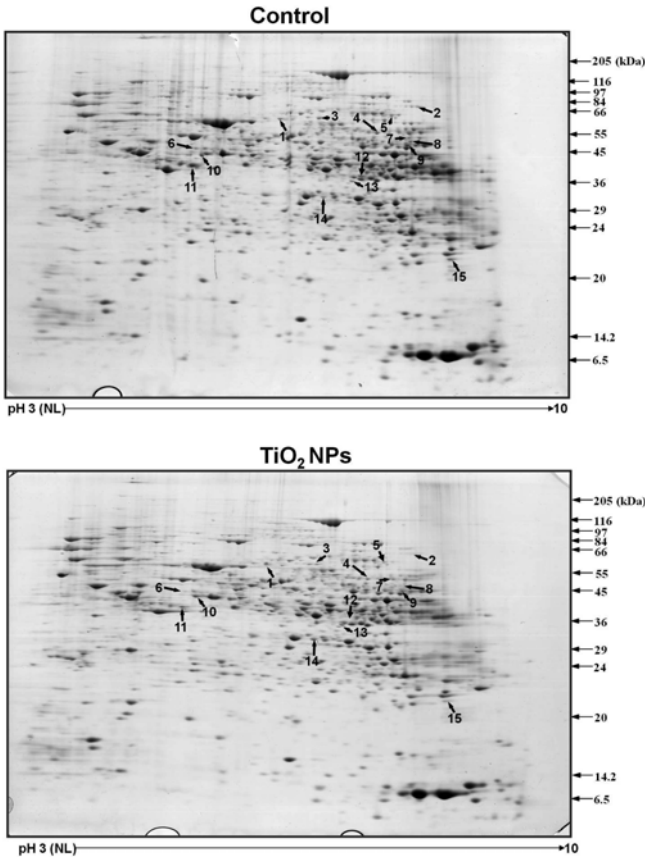

Fig. 1. Representative 2-DE images for mouse liver proteins following exposure to TiO_2 NPs. The protein was separated on 2-DE (pH 3−10) gels and visualized by Coomassie Brilliant Blue staining.

Antioxidative enzyme activity on the gels. Antioxidant enzymes, including CAT and SOD were selected for enzyme activity analysis on the native-PAGE gel. Total activities of CAT and SOD were reduced by TiO_2 NPs, as compared by the band intensity on the activity staining gel (Fig. 4). In particular, two isozymes of SOD, named SOD1 and SOD4, were reduced, whereas the other two isozymes of SOD2 and SOD3 remained constant, in response to TiO_2 NPs.

Discussion

Proteomic techniques were used in the present study to identify the proteins, the expression of which in the mouse liver was altered by the toxicity of TiO_2 NPs. The damages of liver function could be caused by TiO_2 NPs, as evidenced by the increased activities ALT, AST, and ALP (Table 1). When the liver is in dysfunction, the levels of the enzymes rise [Chen *et al*., 2009], and their elevated levels show that the liver could have been injured, and severe inflammatory responses were induced. Moreover, the ratio of ALT/AST, a more

Table 2. Identifications of the altered proteins of mouse liver by LC-MS/MS following exposure to TiO_2 NPs

No.	Identified Protein	Annotation	Score	Cov %	Theoretical MW/pI	Experimental MW/pI	Change
1	Isoform 1 of 60 kDa HSP, mitochondrial precursor (Isoform 1 of HSP60)	IPI00308885.6	250.33	49.01	60955.1/5.91	78832/6.89	↑
2	Fructose-1,6-bisphosphatase 1 (FBP 1)	IPI00228630.5	170.35	43.79	36912.2/6.15	98410/8.50	↘
3	Propionyl-CoA carboxylase alpha chain (PCCA)	IPI00330523.1	280.36	50.14	79921.3/6.83	79921/7.21	↘
4	Electron transfer flavoprotein-ubiquinone oxidoreductasemitochondrial precursor (ETF-QO)	IPI00121322.2	100.30	19.16	68090.6/7.34	60252/8.19	↘
5	Carbonic anhydrase 2 (CA 2)	IPI00121534.11	100.35	57.69	29032.3/6.49	84189/8.28	↘
6	Sulfite oxidase, mitochondiral precursor (SUOX)	IPI00153144.3	90.36	25.27	60755.5/6.07	47316/6.45	↘
7	Arginase-1 (Arg 1)	IPI00117914.3	70.30	34.93	36260.2/6.52	60583/8.34	↘
8	Aldehyde dehydrogenase family 8 member A1 (ALDH 8A1)	IPI00267407.1	190.31	45.79	53663.6/7.50	51532/8.44	↘
9	Catalase (CAT)	IPI00312058.5	128.34	32.26	59764.9/7.72	48754/8.41	↘
10	Elongation factor1-alpha 2 (EF-1 alpha 2)	IPI00119667.1	60.23	13.82	50453.8/9.11	43729/6.48	↘
11	Cytochrome b-c1 complex subunit 1, mitochondrial precursor	IPI00111885.1	120.37	25.42	52768.4/5.81	39221/6.43	↘
12	Apolipoprotein A-1 precursor (Pre-Apo-A1)	IPI00121209.1	140.23	47.73	30587.3/5.64	34957/8.09	↘
13	Isovaleryl-CoA dehydrogenase, mitochondrial precursor (IVD)	IPI00471246.2	110.29	30.42	46325.1/8.53	33133/8.04	↑
14	Beta-ureidopropionase (BUP)	IPI00121639.1	140.30	45.29	43936.8/6.33	29067/7.87	↑
15	Cytochrome b-c1 complex subunit 1, mitochondrial precursor	IPI00111885.1	60.39	17.71	52768.4/5.81	21812/8.76	↘

↘: Down-regulation, ↑: Up-regulation

sensitive indicator for hepatic injury was also enhanced following exposure to TiO_2 NPs; similar data were reported in oral ingestion of nanpoparticles [Wang *et al*., 2007]. ALP was significantly higher than the control group.

Fifteen protein spots, displaying greater than two-fold differences in intensity between control and TiO_2 NP-exposed liver samples, were identified, of which 12 were down-regulated and the remaining 3, up-regulated (Table 2). When using MS/MS, protein scores greater than 45 have been known to be statistically significant [Fu *et al*., 2009]. In Table 2, the experimental molecular weights (MWs) and isoelectric points (pIs) of a few identified proteins are not consistent with their theoretical values, presumably due to a number of factors, including post-translational modification, protein translation from alternatively spliced mRNAs, or oxidative damage [Fu *et al*., 2009].

HSP 60 kDa (HSP 60), essential for the folding and assembly of newly imported proteins, has been implicated in the prevention of protein denaturation under the stress conditions [Cheng *et al*., 1990; Merendino *et al*., 2010]. Therefore, the increased level of isoform 1 of 60 kDa HSP (spot 1) by TiO_2 NPs appears to be associated with a defense mechanism that protects mouse liver from toxicity by TiO_2 NPs. The proteomic result of HSP 60 was in good agreement with the Western blot result.

Fructose-1,6-bisphosphatase is an intermediate in the glycolytic pathway, exerting pharmacological actions on the inflammation by inhibiting cytokine production or interfering with adenosine production. The pharmacological anti-inflammatory activity of fructose-1,6-bisphosphatase was reported to be related with inhibition of the production of inflammatory molecules including reactive oxygen species, prostaglandin E_2, and cycloxygenase 2 expression [Valério *et al*., 2009]. Thus, fructose-1,6-bisphosphatase down-regulation by TiO_2 NPs appears to be related with TiO_2 NPs-induced inflammation in mouse liver.

Propionyl-CoA carboxylase is a key enzyme in the catabolic pathway for the three carbon residues from isoleucine, threonine, valine, branched chain, and odd carbon fatty acids [Hsia *et al*., 1979]. Defects in propionyl-CoA carboxylase are the cause of propionic acidemia type 1 (PA-1). PA-1 is a life-threatening disease characterized by episodic vomiting, neutropenia, periodic thrombocytopenia, and developmental retardation. Furthermore, PA-1 patients have coding sequence mutation in the alpha subunit of propionyl-CoA carboxylase [Campeau *et al*., 1999]. In the present investigation, Propionyl-CoA carboxylase alpha chain, a mitochondrial precursor, was down-regulated by TiO_2 NPs.

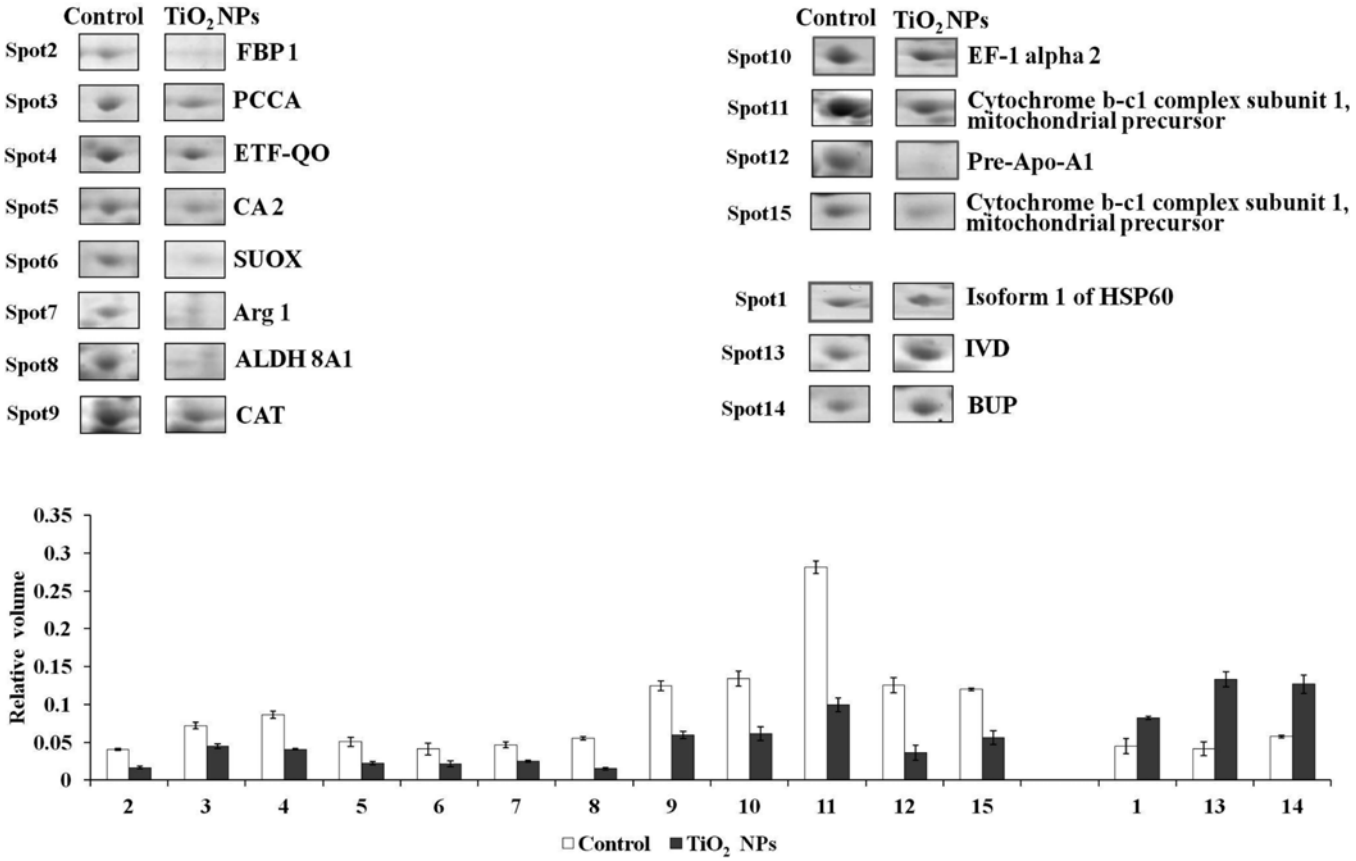

Fig. 2. Zoom-up views of the differentially expressed proteins in rat liver following exposure to TiO_2 NPs. Protein expression levels were determined by relative volume using image analysis. Normalized spot intensities of the TiO_2 NPs versus control group were compared. Mean spot intensities on individual gels are shown.

Carbonic anhydrase catalyzes the reversible reaction involving the hydration of carbon dioxide and the dehydration of carbonic acid [Sugimoto *et al*., 2008]. Carbonic anhydrase is involved in the reduction in tissue pH related with inflammatory pain, as well as the extracellular control of pH in muscle. Apart from aiding the transport of carbon dioxide out of tissues, it was also suggested to serve as an oxygen radical scavenger to protect hepatocytes from oxidation damage [Wong *et al*., 2011]. Exposure to TiO_2 NPs reduced the expression level of carbonic anhydrase 2, suggesting the low protection from TiO_2 NPs-induced hepatocyte damage.

All mammals have large quantities of sulfite oxidase in their liver, kidney, and heart, and very little in their spleen, brain, and blood. Sulfite oxidase oxidizes sulfite into sulfate and, via cytochrome c, transfers the electrons produced to the electron transport chain, allowing generation of ATP [Tan *et al*., 2005]. Some study suggested that sulfite oxidase was found to be only at the priming stage of liver regeneration. Sulfite oxidase is also an important factor for cell apoptosis with cytochrome c [Deng *et al*., 2009]. TiO_2 nanoparticles induced-sulfite oxidase reduction may be associated with reduction in liver regenerative capacity, low ATP production or apoptosis.

Arginase, existing primarily in the liver, hydrolyzes arginine to form urea and ornithine in the urea cycle. There are two arginase isoenzymes encoded by distinct genes in mammalian tissues, known as arginases A1 and A2. Arginase A1 had the highest activity in the liver; however, it played as a key enzyme of the urea cycle. Arginase A1 activity and its mRNA level were significantly decreased in cirrhotic liver, whereas the activity and expression of arginase A2 were concurrently increased, as compared to normal liver [Chrzanowska *et al*., 2009]. Thus, TiO_2 NPs induced-decreased arginase-1 expression also seems to be associated with cirrhosis and carcinoma by TiO_2 NPs.

ALDH are a group of enzymes that catalyze the oxidation of aldehydes, representing a significant metabolic route of aldehyde detoxification. When ALDH is inhibited, it can lead to the accumulation of the reactive electrophiles, which have been shown to modify proteins and lead to increased oxidative stress, mitochondrial dysfunction, and toxicity [Marchitti *et al*., 2010]. ALDH family 8

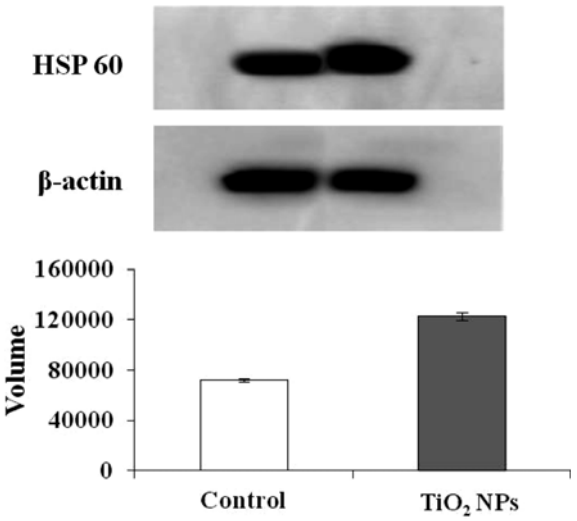

Fig. 3. Validation of differentially regulated mouse liver HSP 60 by Western blot analysis. Band volumes in the Western blots were normalized against β-actin.

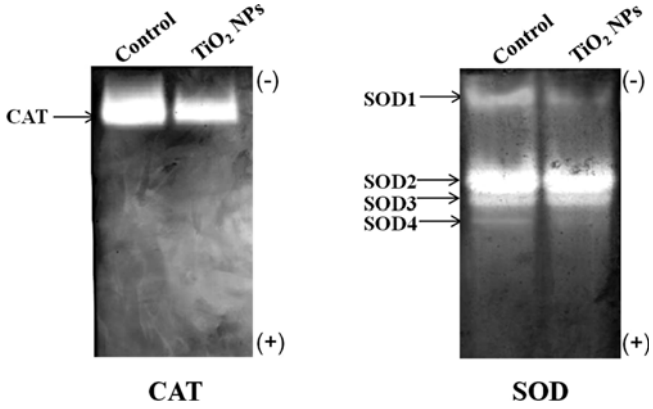

Fig. 4. Changes in the enzyme activities and isozyme patterns for CAT and SOD by TiO_2 NPs.

member A1 was down-regulated by TiO_2 NPs.

Catalase is an antioxidant enzyme that helps the body to convert hydrogen peroxide into water and oxygen, thus prevent free radical damage to the body. Catalase, an enzyme enriched in the hepatocytes and a major determinant of cellular resistance to hydrogen peroxide toxicity was reduced by TiO_2 NPs, indicating a diminished capacity of liver cells to detoxify hydrogen peroxide [Vijayan and Helen, 2007]. Elongation factor-1α (EF-1α) has been shown to be involved in cytoskeletal organization, and it is required for the binding of aminoacyl-tRNAs to the acceptor site of ribosomes during protein synthesis. EF-1α is an important regulator of cell cycle and is over-expressed in tumors of the pancreas, colon, breast, lung, and stomach compared to levels in normal tissue. In addition, over-expression of EF-1α mRNA was correlated with metastasis [Zhu *et al*., 2009]. Recent studies have also correlated the expression of EF-1α2 with survival, tumor size, and p53 mutations [Pecorari *et al*., 2009]. EF-1α2 was down-regulated by TiO_2 NPs in the present investigation.

Cytochrome b-c1 complex is a component of the ubiquiol-cytochrome c reductase complex, which is part of the mitochondrial respiratory chain [Valnot *et al*., 1999]. The cytochrome b-c1 complex is the most widely occurring electron transfer complex capable of energy transduction. The reduction in cytochrome b-c1 complex subunit 1 by TiO_2 NPs could indicate the reduction of energy production in mouse liver.

Apolipoprotein A-1 (Apo A-1) is the major protein component of high-density lipoprotein (HDL), whose protective role in the cardiovascular system has been established [Vuilleumier *et al*., 2004]. Moreover, it was proven that HDL could be a potent inhibitor of pro-inflammatory cytokine production in cell-mediated inflammation. Apo A1 as an anti-inflammatory molecule could block T-cell signals from macrophages and inhibit the production of tumor necrosis factor alpha (TNF-α) and interleukin-1 [Hyka *et al*., 2001]. Thus, the marked decrease in Apo A1 precursor level in the present study may suggest the elevated inflammation after exposure to TiO_2 NPs.

Isovaleryl-CoA dehydrogenase is a mitochondrial flavoenzyme, which catalyzes the conversion of isovaleryl-CoA into 3-methylcrotonyl-CoA. This enzyme belongs to the family of oxidoreductases, specifically those acting on the CH-CH group of donor with other acceptors, and are a member of acyl-CoA dehydrogenases family [Bachhawat *et al*., 1956]. Deficiency of isovaleryl-CoA dehydrogenase activity in human causes isovaleric acidemia [Mohsen *et al*., 1998]. Isovaleryl-CoA dehydrogenase was up-regulated by TiO_2 nanoparticles in this study.

The reactive oxygen species (ROS) generation was reported to be caused by the chemical properties of TiO_2 NPs [Cui *et al*., 2011]. Overproduction of ROS breaks down the balance of oxidative/antioxidative system in the liver, resulting in the lipid peroxidation and hepatocyte apoptosis of mice, which may be closely associated with alterations of antioxidative enzyme levels. When antioxidative enzyme was inhibited, it led to enhanced oxidative stress, mitochondrial dysfunction, and toxicity [Allen *et al*., 2010]. In the present study, total activities of CAT and SOD were inhibited and the isozyme pattern for SOD was changed after exposure to TiO_2 NPs.

Moreover, 15 proteins were differentially expressed by TiO_2 NPs, among which, ALDH, catalase, and propionyl-CoA carboxylase alpha proteins, that were detected in the present study by TiO_2 NPs, were also reported to be

differentially expressed by ethanol-dependent hepatotoxicity [Venkatraman *et al*., 2004; Newton *et al*., 2009; Andringa *et al*., 2010], and apolipoprotein A-1 and EF-1 protein, which were reported in drug-induced (acetaminophen, amiodarone, and cyclosporine A) hepatotoxicity [Van Summeren *et al*., 2011], were also detected in the present study.

Taken together, the present data raise an important possibility that the differentially expressed proteins could be involved in the hepatotoxicity by TiO_2 NPs.

References

Allen EM, Anderson DG, Florang VR, Khanna M, Hurley TD, and Doorn JA (2010) Relative inhibitory potency of molinate and metabolites with aldehyde dehydrogenase 2: Implications for the mechanism of enzyme inhibition. *Chem Res Toxicol* **23**, 1843–1850.

Andringa KK, King AL, Eccleston HB, Mantena SK, Landar A, Jhala NC, Dickinson DA, Squadrito GL, and Bailey SM (2010) Analysis of the liver mitochondrial proteome in response to ethanol and S-adenosylmethionine treatments: Novel molecular targets of disease and hepatoprotection. *Am J Physiol Gastrointest Liver Physiol* **298**, G732–G745.

Bachhawat BK, Robinson WG, and Coon MJ (1956) Enzymatic carboxylation of beta-hydroxyisovaleryl coenzyme A. *J Biol Chem* **219**, 539–550.

Campeau E, Dupuis L, León-Del-Rio A, and Gravel R (1999) Coding sequence mutations in the alpha subunit of propionyl-CoA carboxylase in patients with propionic acidemia. *Mol Genet Metab* **67**, 11–22.

Chen J, Dong X, Zhao J, and Tang G (2009) In vivo acute toxicity of titanium dioxide nanoparticles to mice after intraperitioneal injection. *J Appl Toxicol* **29**, 330–337.

Cheng MY, Hartl FU, and Horwich AL (1990) The mitochondrial chaperonin hsp60 is required for its own assembly. *Nature* **348**, 455–458.

Chrzanowska A, Gajewska B, and Barañczyk-KuŸma A (2009) Arginase isoenzymes in human cirrhotic liver. *Acta Biochim Pol* **56**, 465–469.

Cui Y, Gong X, Duan Y, Li N, Hu R, Liu H, Hong M, Zhou M, Wang L, Wang H, and Hong F (2010) Hepatocyte apoptosis and its molecular mechanisms in mice caused by titanium dioxide nanoparticles. *J Hazard Mater* **183**, 874–880.

Cui Y, Liu H, Zhou M, Duan Y, Li N, Gong X, Hu R, Hong M, and Hong F (2011) Signaling pathway of inflammatory responses in the mouse liver caused by TiO_2 naoparticles. *J Biomed Mater Res A* **96**, 221–229.

Deng X, Li W, Chen N, Sun Y, Wei H, Jiang Y, and He F (2009) Exploring the priming mechanism of liver regeneration: Proteins and protein complexes. *Proteomics* **9**, 2202–2216.

Fu Q, Liu PC, Wang JX, Song QS, and Zhao XF (2009) Proteomic identification of differentially expressed and phosphorylated proteins in epidermis involved in larval-pupal metamorphosis of *Helicoverpa armigera*. *BMC Genomics* **10**, 600.

Hsia YE, Scully KJ, and Rosenberg LE (1979) Human propionyl CoA carboxylase: some properties of the partially purified enzyme in fibroblasts from controls and patients with propionic acidemia. *Pediatr Res* **13**, 746–751.

Hyka N, Dayer JM, Modoux C, Kohno T, Edwards CK 3rd, Roux-Lombard P, and Burger D (2001) Apolipoprotein A-I inhibits the production of interleukin-1beta and tumor necrosis factor-alpha by blocking contact-mediated activation of monocytes by T lymphocytes. *Blood* **97**, 2381–2389.

Jeon YM, Park SK, Rhee SK, and Lee MY (2010) Proteomic profiling of the differentially expressed proteins by TiO_2 nanoparticles in mouse kidney. *Mol Cell Toxicol* **6**, 419–425.

Jeon YM, Son BS, and Lee MY (2011) Proteomic identification of the differentially expressed proteins in human lung epithelial cells by airborne particulate matter. *J Appl Toxicol* **31**, 45–52.

Linnainmaa K, Kivipensas P, and Vainio H (1997) Toxicity and cytogenetic studies of ultrafine titanium dioxide in cultured rat liver epithelial cells. *Toxicol In Vitro* **11**, 329–335.

Ma L, Zhao J, Wang J, Liu J, Duan Y, Liu H, Li N, Yan J, Ruan J, Wang H, and Hong F (2009) The acute liver injury in mice caused by nano-anatase TiO_2. *Nanoscale Res Lett* **4**, 1275–1285.

Marchitti SA, Brocker C, Orlicky DJ, and Vasiliou V (2010) Molecular characterization, expression analysis, and role of ALDH3B1 in the cellular protection against oxidative stress. *Free Radic Biol Med* **49**, 1432–1443.

Merendino AM, Bucchieri F, Campanella C, Marcianò V, Ribbene A, David S, Zummo G, Burgio G, Corona DF, Conway de Macario E, Macario AJ, and Cappello F (2010) Hsp60 is actively secreted by human tumor cells. *PLoS One* **5**, e9247.

Mohsen AW, Anderson BD, Volchenboum SL, Battaile KP, Tiffany K, Roberts D, Kim JJ, and Vockley J (1998) Characterization of molecular defects in isovaleryl-CoA dehydrogenase in patients with isovaleric acidemia. *Biochemistry* **37**, 10325–10335.

Newton BW, Russell WK, Russell DH, Ramaiah SK, and Jayaraman A (2009) Liver proteome analysis in a rodent model of alcoholic steatosis. *J Proteome Res* **8**, 1663–1671.

Park EJ, Yoon JH, Choi KH, Yi JH, and Park KS (2009) Induction of chronic inflammation in mice treated with titanium dioxide nanoparticles by intratracheal instillation. *Toxicology* **260**, 37–46.

Park SK, Jeon YM, Son BS, Youn HS, and Lee MY (2011) Proteomic analysis of the differentially expressed proteins by airborne nanoparticles. *J Appl Toxicol* **31**, 463–470.

Passadore I, Iadarola P, Di Poto C, Giuliano S, Montecucco C, Cavagna L, Bonino C, Meloni F, Fietta AM, Lisa A, Salvini R, and Bardoni AM (2009) 2-DE and LC-MS/MS for a comparative proteomic analysis of BALf from subjects with different subsets of inflammatory myopathies. *J*

Proteome Res **8**, 2331–2340.

Pecorari L, Marin O, Silvestri C, Candini O, Rossi E, Guerzoni C, Cattelani S, Mariani SA, Corradini F, Ferrari-Amorotti G, Cortesi L, Bussolari R, Raschellà G, Federico MR, and Calabretta B (2009) Elongation Factor 1 alpha interacts with phospho-Akt in breast cancer cells and regulates their proliferation, survival and motility. *Mol Cancer* **8**, 58.

Sohaebuddin SK, Thevenot PT, Baker D, Eaton JW, and Tang L (2010) Nanomaterial cytotoxicity is composition, size, and cell type dependent. *Part Fibre Toxicol* **7**, 22.

Sugimoto A, Ikeda H, Tsukamoto H, Kihira K, Takeda C, Hirose J, Hata T, Baba E, and Ono Y (2008) The mechanisms by which latanoprost free acid inhibits human carbonic anhydrase I and II. *Biol Pharm Bull* **31**, 796–801.

Tan WH, Eichler FS, Hoda S, Lee MS, Baris H, Hanley CA, Grant PE, Krishnamoorthy KS, and Shih VE (2005) Isolated sulfite oxidase deficiency: A case report with a novel mutation and review of the literature. *Pediatrics* **116**, 757–766.

Valério DA, Ferreira FI, Cunha TM, Alves-Filho JC, Lima FO, De Oliveira JR, Ferreira SH, Cunha FQ, Queiroz RH, and Verri WA Jr (2009) Fructose-1,6-bisphosphate reduces inflammatory pain-like behaviour in mice: Role of adenosine acting on A1 receptors. *Br J Pharmacol* **158**, 558–568.

Valnot I, Kassis J, Chretien D, de Lonlay P, Parfait B, Munnich A, Kachaner J, Rustin P, and Rötig A (1999) A mitochondrial cytochrome b mutation but no mutations of nuclearly encoded subunits in ubiquinol cytochrome c reductase (complex III) deficiency. *Hum Genet* **104**, 460–466.

Van Summeren A, Renes J, Bouwman FG, Noben JP, van Delft JH, Kleinjans JC, and Mariman EC (2011) Proteomics investigations of drug-induced hepatotoxicity in HepG2 cells. *Toxicol Sci* **120**, 109–122.

Venkatraman A, Landar A, Davis AJ, Chamlee L, Sanderson T, Kim H, Page G, Pompilius M, Ballinger S, Darley-Usmar V, and Bailey SM (2004) Modification of the mitochondrial proteome in response to the stress of ethanol-dependent hepatotoxicity. *J Biol Chem* **279**, 22092–22101.

Vijayan V and Helen A (2007) Protective activity of *Bacopa monniera* Linn. on nicotine-induced toxicity in mice. *Phytother Res* **21**, 378–381.

Vuilleumier N, Reber G, James R, Burger D, de Moerloose P, Dayer JM, and Roux-Lombard P (2004) Presence of autoantibodies to apolipoprotein A-1 in patients with acute coronary syndrome further links autoimmunity to cardiovascular disease. *J Autoimmun* **23**, 353–360.

Wang J, Zhou G, Chen C, Yu H, Wang T, Ma Y, Jia G, Gao Y, Li B, Sun J, Li Y, Jiao F, Zhao Y, and Chai Z (2007) Acute toxicity and biodistribution of different sized titanium dioxide particles in mice after oral administration. *Toxicol Lett* **168**, 176–185.

Wong LL, Fan ST, Man K, Sit WH, Jiang PP, Jor IW, Lee CY, Ling WL, Tam KT, and Wan JM (2011) Identification of liver proteins and their roles associated with carbon tetrachloride-induced hepatotoxicity. *Hum Exp Toxicol* **30**, 1369–1381.

Xiong D, Fang T, Yu L, Sima X, and Zhu W (2011) Effects of nano-scale TiO_2, ZnO and their bulk counterparts on zebrafish: acute toxicity, oxidative stress and oxidative damage. *Sci Total Environ* **409**, 1444–1452.

Xu J, Futakuchi M, Iigo M, Fukamachi K, Alexander DB, Shimizu H, Sakai Y, Tamano S, Furukawa F, Uchino T, Tokunaga H, Nishimura T, Hirose A, Kanno J, and Tsuda H (2010) Involvement of macrophage inflammatory protein 1 alpha (MIP1alpha) in promotion of rat lung and mammary carcinogenic activity of nanoscale titanium dioxide particles administered by intra-pulmonary spraying. *Carcinogenesis* **31**, 927–935.

Zhu G, Yan W, He HC, Bi XC, Han ZD, Dai QS, Ye YK, Liang YX, Wang J, and Zhong W (2009) Inhibition of proliferation, invasion, and migration of prostate cancer cells by downregulating elongation factor-1alpha expression. *Mol Med* **15**, 363–370.